

Intensification of bubble columns by vibration excitement

J. Ellenberger, J.M. van Baten, R. Krishna*

Department of Chemical Engineering, University of Amsterdam, Nieuwe Achtergracht 166, 1018 WV Amsterdam, The Netherlands

Abstract

In this paper we show that application of low-frequency vibrations, in the 40–120 Hz range, to the liquid phase of an air–water bubble column causes significantly smaller bubbles to be generated at the nozzle. In experiments with a single capillary nozzle, the bubble size is reduced by about 40–50%, depending on the vibration frequency and amplitude. CFD simulations show that the vibrations tend to lead to earlier detachment of the bubbles from the nozzles, leading to smaller bubble sizes.

Using a 12-capillary nozzle arrangement, the gas holdup, ε , was measured for a range of superficial gas velocities. Application of vibrations to the liquid phase leads to a significant increase in the gas holdup. The increase in the gas holdup is attributed mainly to a significant reduction in the rise velocity of the bubble swarm due to the generation of standing waves in the column. Furthermore, application of vibrations to the liquid phase serves to stabilize the homogenous bubbly flow regime and delay the onset of the churn-turbulent flow regime.

© 2003 Elsevier Science B.V. All rights reserved.

Keywords: Bubble column; Vibration excitement; Process intensification; Gas holdup; Standing waves

1. Introduction

A bubble column reactor is commonly used in the process industries for carrying out a variety of liquid phase reactions [1]. There are two regimes of operation for a bubble column. At low superficial gas velocities, U , we have homogeneous bubbly flow in which the dispersion consists of bubbles that are roughly uniform in size. Homogeneous bubbly flow is sustainable up to a superficial gas velocity $U = U_{\text{trans}}$, called the transition gas velocity. When U is increased to values beyond U_{trans} , we enter the heterogeneous or churn-turbulent flow regime. In this churn-turbulent flow regime, we have a wide distribution of bubble sizes, ranging from 3 to 50 mm depending on the system properties [2]. The wide

distribution of bubble sizes causes a wide gas phase residence time distribution; this is often detrimental to reactor conversion and selectivity.

Uniformity of bubble sizes in gas–liquid reactors can be achieved by means of mechanical agitation or *stirring*. However, the stirring action of the agitator causes intense backmixing of both liquid and gas phases. In some biotechnological applications, the high shear, experienced near the agitator, is undesirable. The major objective of the present communication is to demonstrate the advantages of a *shaken* or vibrated bubble column reactor in which the liquid phase is subjected to low-frequency vibrations in the 40–120 Hz range. A special vibration excitement device is used for this purpose. The advantage of using low-frequency vibrations over mechanical agitation is that the plug flow character of the bubbles is maintained and no additional large-scale backmixing of the liquid phase is induced.

* Corresponding author. Tel.: +31-20-525-7007;

fax: +31-20-525-5604.

E-mail address: krishna@science.uva.nl (R. Krishna).

There is some evidence in the published literature to show that the application of vibrations to the liquid phase, at frequencies of the order of 100 Hz, can (a) influence bubble rise in gas–liquid dispersions [3,4]; (b) reduce the bubble size [5,6]; and (c) improve gas–liquid mass transfer [7–11]. Vibrations have found to have a beneficial effect in gas–solids fluidization [12,13]. Our present work extends the published works in bubble columns to high superficial gas velocities in order to show that application of vibrations helps to stabilize the homogeneous bubble flow regime and results in a more uniform dispersion of smaller sized bubbles.

2. Experimental set-up and procedures

The experimental set-up consists of a bubble column, a vibration exciter, a power amplifier, a vibra-

tion controller and a personal computer. A schematic diagram of the experimental set-up is given in Fig. 1. The bubble column, made of polyacrylate, has an inner diameter of 0.10 m and a height of 2.0 m. The bottom of the column is sealed by a silicon rubber membrane of 0.4 mm thickness, clamped between two metal disks of 0.096 m in diameter; see inset to Fig. 1. At a distance of 0.1 m above the membrane, air is fed to the bubble column through two types of gas distributors: (a) a single capillary of 0.9 mm i.d. (see inset on left of Fig. 1), and (b) 12 stainless steel capillaries of 0.9 mm i.d. (see inset on the right of Fig. 1). Stainless steel high-pressure pre-filters with pores of 2 μm are placed at the inlet of the capillaries resulting in a high-pressure drop restriction between the gas supply annulus and the capillaries, which in turn results in a constant gas flow. The gas flow is controlled by means of a calibrated flow meter (*Brooks*). In order to maintain the membrane at constant horizontal

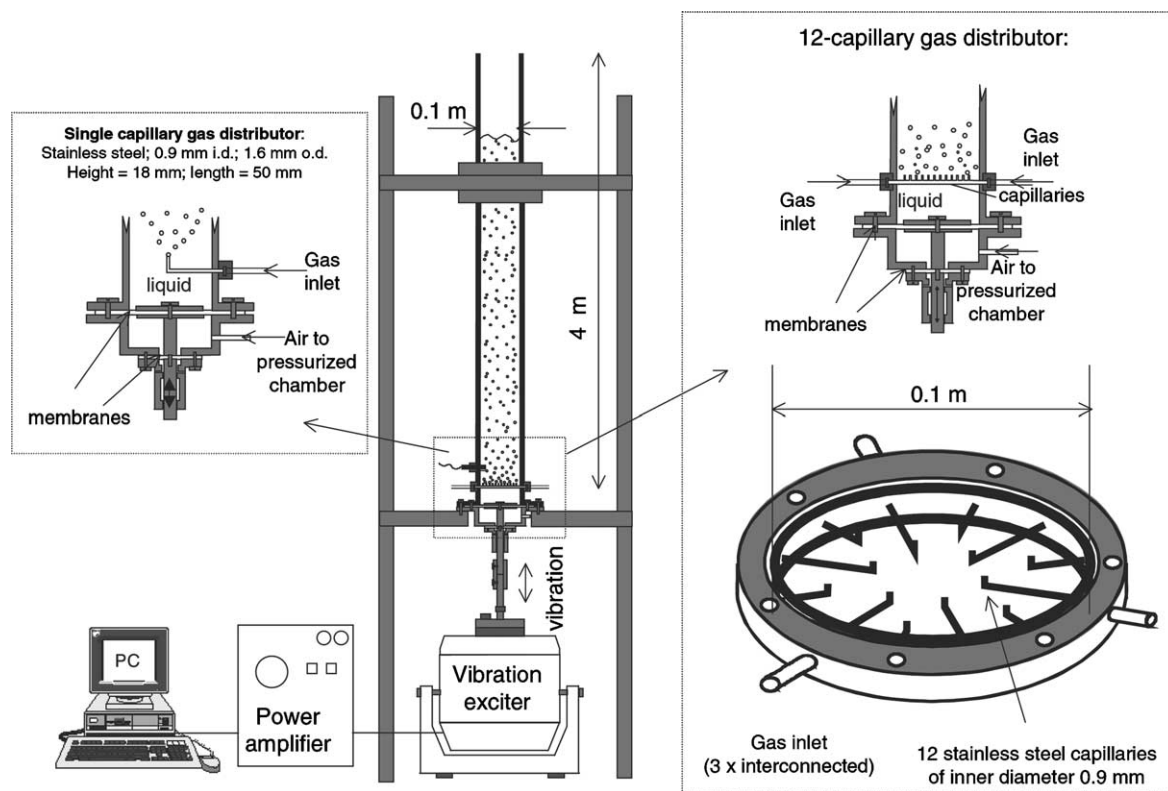


Fig. 1. Experimental set-up of the bubble column with vibration excitation device. Further details of the experimental set-up including photographs of the rig are to be found on our website: <http://ct-cr4.chem.uva.nl/vibrationexciter>.

position after filling the column with the liquid phase, a chamber for pressure compensation is mounted below the membrane. The membrane is connected to an air-cooled vibration exciter (*TIRAvib 5220*, Germany). The amplifier of this vibration exciter is controlled by the *SignalCalc 550 Vibration controller* in a PC environment. The frequency range is 10–5000 Hz. Depending on the frequency, the amplitude can be varied between 0 and 25 mm. The vibrations follow a sinusoidal motion. The maximum acceleration under unloaded conditions is 700 m s^{-2} . For mass transfer measurements, an oxygen electrode (*Yellow Springs Incorporated*) is placed in the bubble column at a distance of 0.1 m above the gas distributor in such a way that the gas bubbles did not hit the electrode. Further details of the experimental set-up including photographs of the rig are to be found on our website: <http://ct-cr4.chem.uva.nl/vibrationexciter/>.

With the single capillary gas inlet device, bubble sizes were measured for a range of vibration frequencies and inlet gas velocities. At each vibration frequency, video recordings, using a Panasonic DSP colour CCD camera, of the air–water or oil–water dispersion were made at 25 frames/s for a period of 5 s. Frame-by-frame analysis of the video images gives accurate information on the number of bubbles passing through the observation window in the time interval of the observation (5 s). The video imaging technique is the same as that described in our earlier publication [6]. For the set volumetric flow rate of the dispersed phase, the average air bubble diameter of the dispersion can be calculated.

With the 12-capillary gas inlet device, the gas holdup has been measured for varying conditions of vibration frequency, vibration amplitude and the superficial gas velocity U in the column. All the measurements have been carried out at room temperature with air as the gas phase and dematerialized water as the liquid phase. The pressure at the top of the column is atmospheric. The gas holdup ε is measured by visually recording the dispersion height H above the gas distributor; the gas holdup is then calculated from

$$\varepsilon = 1 - \frac{H_0}{H} \quad (1)$$

where H_0 is the height of the ungasged liquid in the column.

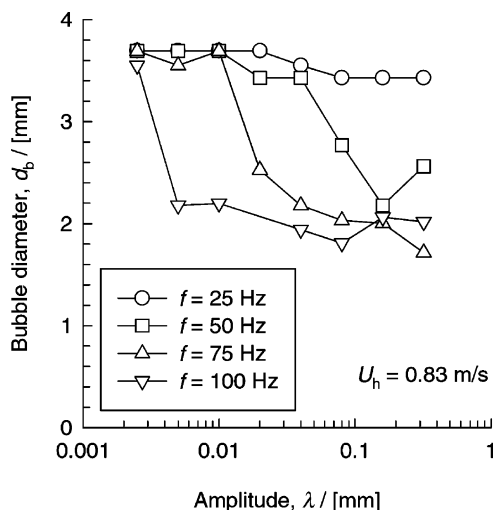


Fig. 2. Influence of vibration frequency f and amplitude λ on the bubble diameter for hole velocity $U_h = 0.83 \text{ m/s}$.

3. Bubble size with single capillary distributor

In the first set of experiments, the air flow rate through the single capillary was maintained at $5.3 \times 10^{-7} \text{ m}^3/\text{s}$ which corresponds to a hole velocity in the capillary, $U_h = 0.83 \text{ m/s}$. Bubble sizes were measured for a range of frequencies, $f = 25, 50, 75$ and 100 Hz , and vibration amplitudes, $\lambda = 0.0025\text{--}0.32 \text{ mm}$. These measurements were carried out taking the clear height of water in the column $H_0 = 0.5 \text{ m}$. The measured bubble sizes are plotted in Fig. 2. For a vibration frequency of 25 Hz , there is very little reduction in the bubble size. When the f is increased to 50 Hz , we note a reduction in bubble size, provided λ is higher than about 0.1 mm . At $f = 75 \text{ Hz}$, λ should be higher than 0.05 mm for a significant reducing effect on the bubble size. At $f = 100 \text{ Hz}$ we observe a significant reduction in bubble size for $\lambda > 0.008 \text{ mm}$.

In order to understand the influence of vibrations on the bubble size, we need to consider the physics of the bubble formation process. We undertook CFD simulations of the bubble formation process using the volume-of-fluid technique, described in our earlier publication [14]. Further computational details, along with details of the numerical procedure and grid used can be found on our website <http://ct-cr4.chem.uva.nl/sonicsim/>. First, we performed VOF simulations

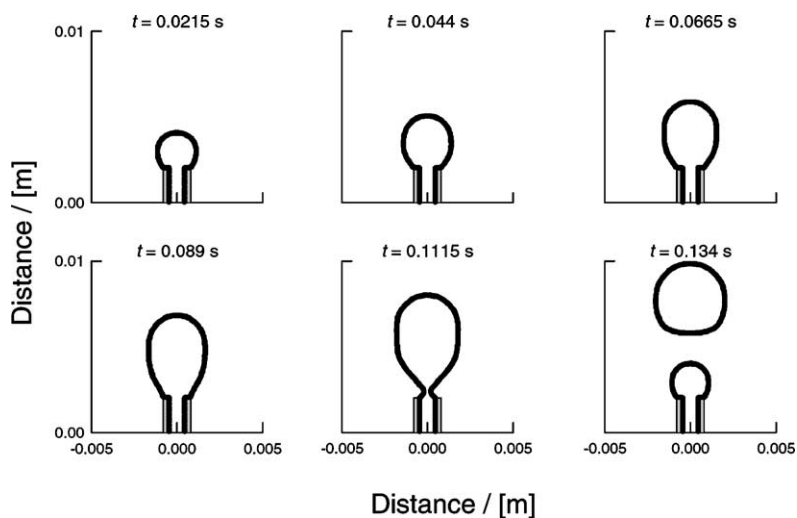


Fig. 3. VOF simulations of bubble formation at a single orifice of internal diameter 0.9 mm. Snapshots for $U_h = 0.5$ m/s and no vibrations. Animations can be viewed on our website: <http://ct-cr4.chem.uva.nl/capillary/>.

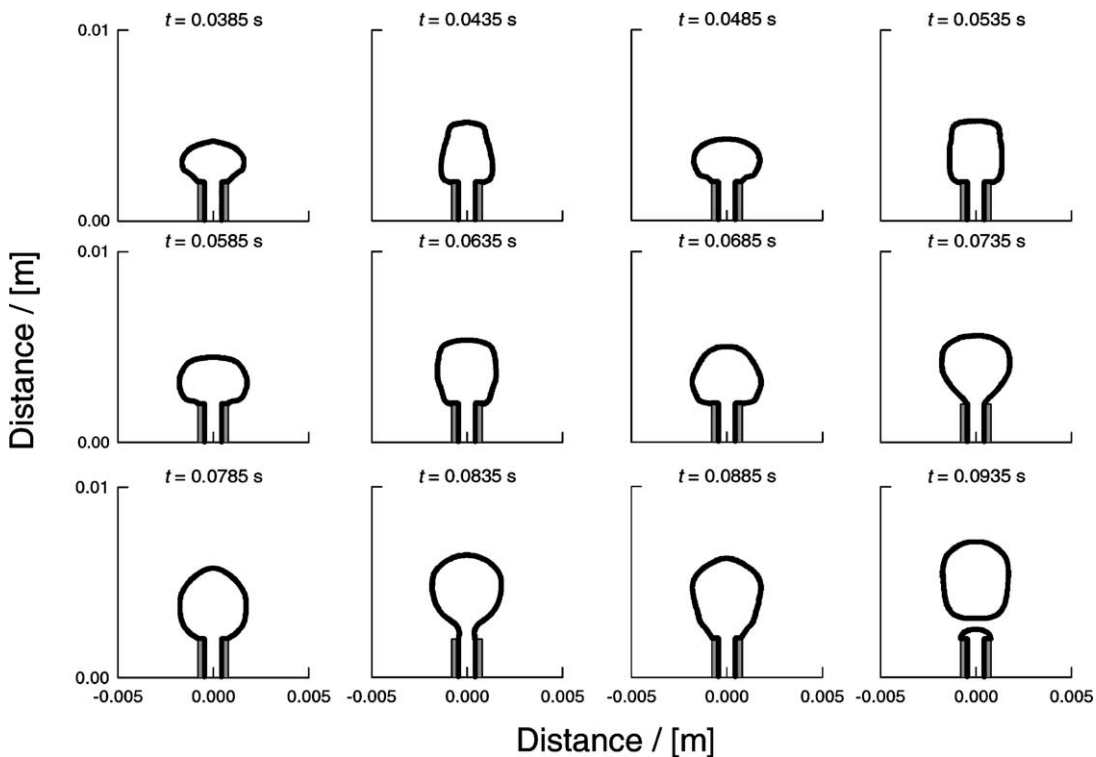


Fig. 4. VOF simulations of bubble formation at a single orifice of internal diameter 0.9 mm. Snapshots for $U_h = 0.5$ m/s, $f = 100$ Hz, and $\lambda = 1$ mm. Animations can be viewed on our website: <http://ct-cr4.chem.uva.nl/sonicsim/>.

for the no-vibrations case. Snapshots of bubble formation at the orifice (nozzle velocity $U_h = 0.5$ m/s) at different time steps are shown in Fig. 3. The bubble size is determined by a balance between the surface tension forces (that prevent the bubble from breaking) and the buoyancy force (that favors detachment). At $t = 0.1115$ s, these two forces are practically equal to each other. Further increase in bubble size tends to increase the buoyancy and the bubble detaches because the surface tension forces are exceeded by the buoyancy; this happens before $t = 0.134$ s. The animations of the bubble formation and detachment can be seen on our website: <http://ct-cr4.chem.uva.nl/capillary/>.

Now, let us consider the situation where the liquid phase at the bottom is subjected to a sinusoidal wave motion following $\lambda \sin(2\pi t)$, where t is the time. Snapshots of the simulation for various values of t are shown in Fig. 4 for $U_h = 0.5$ m/s; $f = 100$ Hz and $\lambda = 0.2$ mm; animations can be viewed on our website: <http://ct-cr4.chem.uva.nl/sonicsim/>. The influence of the vibrations is evident; the growing bubble flaps up and down. Vibrations tend to help overcome the surface tension forces and therefore the bubble detaches “earlier” from the capillary nozzle. In this simulation, we note that the detachment occurs at $t = 0.0935$ s, significantly earlier than for the no-vibrations case (see Fig. 3). Due to earlier detachment from the orifice, the resulting bubble sizes are smaller.

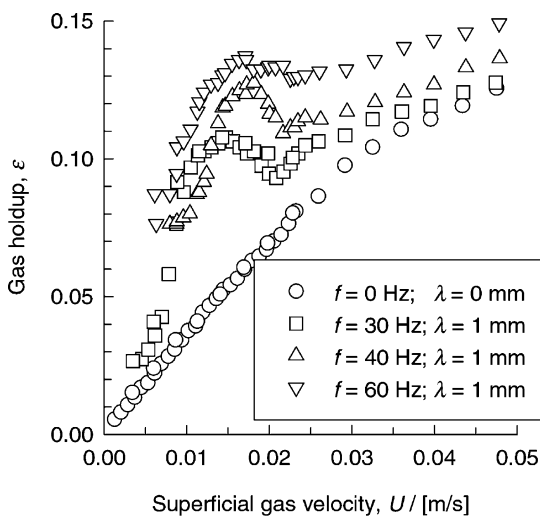


Fig. 5. Gas holdup, with and without vibrations.

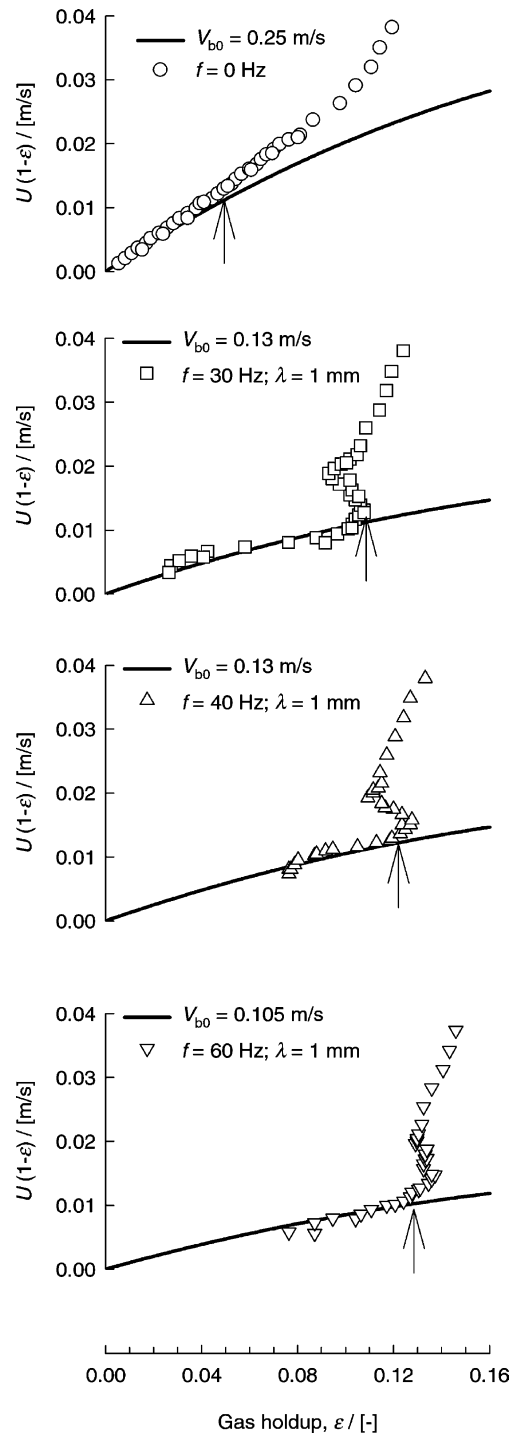


Fig. 6. Wallis plot for the set of holdup measurements shown in Fig. 5.

4. Gas holdup measurements with 12-capillary distributor

We now consider the influence of vibrations on the gas holdup in the 0.1 m diameter column using the 12-capillary gas distributor device. For a range of superficial gas velocities, U , the gas holdup was measured for the no-vibrations case along with three cases in which the vibration frequencies were set at 30, 40 and 60 Hz at a constant amplitude $\lambda = 1$ mm and clear liquid height $H_0 = 1.10$ m; the results are shown in Fig. 5. Depending on the operating conditions, the improvement in the gas holdup is in the 0–300% range. Below a vibration frequency of 20 Hz, there is no improvement in the gas holdup; the higher the vibration frequency beyond 30 Hz, the higher is the gas holdup.

In order to gain further insight into the reasons behind the increase of gas holdup due to application of the vibrations to the liquid phase, we adopt the drift-flux analysis of Wallis [15] for the holdup experiments. The Wallis drift-flux is defined as $V_{\text{slip}}\varepsilon(1-\varepsilon)$ where V_{slip} is the slip velocity between the gas and liquid phases. For a bubble column with no net liquid flow, $V_{\text{slip}} = U/\varepsilon$. The Richardson and Zaki [16] expression for the slip velocity is given by

$$V_{\text{slip}} = V_{b0}(1-\varepsilon)^{n-1} \quad (2)$$

where V_{b0} is the single-bubble rise velocity and n is the Richardson–Zaki index. The factor $(1-\varepsilon)^{n-1}$

in Eq. (2) describes the hindering effect of the rising bubble swarm. In Fig. 6, we plot $V_{\text{slip}}\varepsilon(1-\varepsilon) \equiv U(1-\varepsilon)$ against ε for the set of experiments shown in Fig. 5 with varying vibration frequencies. Also shown in Fig. 6 are calculations using Eq. (2), shown by the continuous lines drawn taking the Richardson–Zaki index $n = 2$ (a typical value for air–water systems) and a fitted value for V_{b0} for the data points with low gas holdups. The point of departure of the experimental data points from Eq. (2) signifies the regime transition point (holdup $\varepsilon_{\text{trans}}$, superficial gas velocity U_{trans}). The regime transition holdup $\varepsilon_{\text{trans}}$ is plotted in Fig. 8 as a function of the vibration frequency. It is clear that application of vibrations tends to delay the transition to the heterogeneous flow regime. A snapshot of the column operation at $U = 0.017$ m/s, without application of vibration is shown in Fig. 7(a). The operation is clearly in the heterogeneous flow regime, as is evidenced by the presence of a few “large” bubbles. The corresponding snapshot for column operation with a vibration frequency $f = 60$ Hz and amplitude $\lambda = 1$ mm is shown in Fig. 7(b). The bubbles are significantly smaller in size and the dispersion is uniform.

The fitted value of V_{b0} , the single-bubble rise velocity, is plotted against f in Fig. 8. For the no-vibrations case the value of $V_{b0} = 0.25$ m/s which is a typical value for air–water systems with bubbles in the 3–7 mm size range. The value of V_{b0} reduces to values in the range 0.105–0.13 m/s on application of

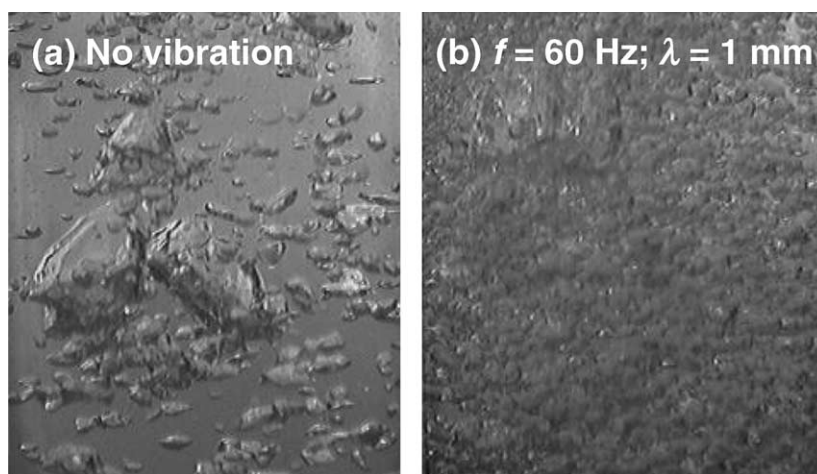


Fig. 7. Snapshots of the column operation with 12-capillary gas distributor operating at a superficial gas velocity $U = 0.017$ m/s and liquid column height $H_0 = 1.10$ m. (a) Column operating without vibration excitement. (b) Operation with vibration $f = 60$ Hz and $\lambda = 1$ mm.

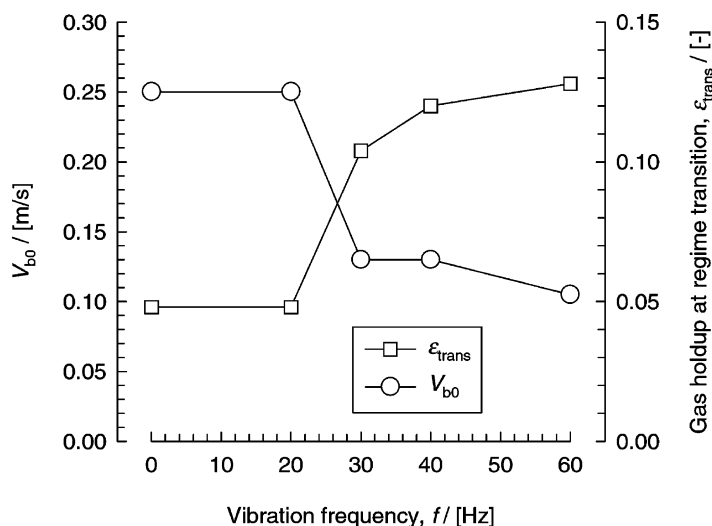


Fig. 8. Variation of ϵ_{trans} and V_{b0} with the vibration frequency f .

vibration. This significant reduction in the rise velocity of the bubble size cannot be attributed to the reduction in the bubble size. For air–water systems, the single-bubble rise velocity is practically independent of the bubble size for d_b values in the 3–7 mm size range [17,18]. The inescapable conclusion, therefore, is that the vibrations to the liquid phase have the effect of reducing the rise velocity of the bubble swarm due to the creation of standing waves.

5. Conclusions

The following major conclusions can be drawn from our study:

- low-frequency vibrations, in the 40–120 Hz range, are capable of causing a 40–50% reduction in the bubble sizes formed at a single capillary;
- VOF simulations of bubble formation at a single capillary shows that vibrations facilitate bubble detachment from the orifice, leading to smaller bubble sizes;
- compared to the no-vibrations case the gas holdup can be increased by a factor of about 2 (see Fig. 5);
- application of vibrations tends to delay the transition to the churn-turbulent flow regime (see Fig. 8);

- the increase in the gas holdup is largely to be attributed to the reduction in the rise velocity of the bubble swarm due to the generation of standing waves.

The energy requirement for vibrations is estimated to be an order of magnitude lower than that for stirred vessels. It is concluded that application of low-frequency vibrations has the potential of improving the gas–liquid contacting in bubble columns.

Acknowledgements

This research was supported by a grant from The Netherlands Foundation for Scientific Research (NWO) for development of novel concepts in reactive separations technology.

References

- W.D. Deckwer, *Bubble Column Reactors*, Wiley, New York, 1992.
- J.W.A. de Swart, R.E. van Vliet, R. Krishna, *Chem. Eng. Sci.* 51 (1996) 4619–4629.
- G.J. Jameson, J.F. Davidson, *Chem. Eng. Sci.* 21 (1966) 29–34.
- G.J. Jameson, *Chem. Eng. Sci.* 21 (1966) 35–48.
- L. Grinis, Y. Monin, *Chem. Eng. Technol.* 5 (1999) 439–442.

- [6] R. Krishna, J. Ellenberger, M.I. Urseanu, F.J. Keil, *Naturwissenschaften* 87 (2000) 455–459.
- [7] M.H.I. Baird, *Chem. Eng. Sci.* 18 (1963) 685–687.
- [8] A. Bartsch, *Z. Naturforsch.* 50 (1995) 228–234.
- [9] K.L. Harbaum, G. Houghton, *Chem. Eng. Sci.* 13 (1960) 90–92.
- [10] N.O. Lemcoff, G.J. Jameson, *AIChEJ* 21 (1975) 730–735.
- [11] R. Krishna, J. Ellenberger, *Int. J. Multiphase Flow* 28 (2002) 1223–1234.
- [12] C.A. Herrera, E.K. Levy, *AIChEJ* 48 (2002) 503–513.
- [13] K. Noda, Y. Mawatari, S. Uchida, *Powder Technol.* 99 (1998) 11–14.
- [14] R. Krishna, M.I. Urseanu, J.M. van Baten, J. Ellenberger, *Chem. Eng. Sci.* 54 (1999) 171–183.
- [15] G.B. Wallis, *One-dimensional Two Phase Flow*, McGraw-Hill, New York, 1969.
- [16] J.F. Richardson, W.N. Zaki, *Trans. Inst. Chem. Eng.* 32 (1954) 35–53.
- [17] R. Clift, J.R. Grace, M.E. Weber, *Bubbles, Drops and Particles*, Academic Press, San Diego, 1978.
- [18] R. Krishna, M.I. Urseanu, J.M. van Baten, J. Ellenberger, *Int. Commun. Heat Mass Transfer* 26 (1999) 781–790.